Adaptive coded modulation under noisy channel state information and antenna diversity

Duc V. Duong

Norwegian Defence Research Establishment (FFI)

5 February 2007

FFI-rapport 2007/00346

1028

ISBN 978-82-464-1109-5

Keywords

Adaptiv kodet modulasjon (ACM)

Pilot-assitert modulasjon (PSAM)

Antennediversitet og diversitetskombinering

Estimerings- og prediksjonsfeil

Optimal pilotavstand

Optimal effektfordeling

Approved by

Vidar S. Andersen Avdelingssjef/Director

Sammendrag

Rapporten omhandler analyse og optimalisering av single-carrier adaptiv kodet modulasjonssystemer med antennediversitet hvor multidimensjonal trellis koder er brukt som komponentkoder.

Både estimerings- og prediksjonsfeil er tatt hensyn til i analysen. For å kunne estimere og prediktere kanalen benyttes det en metode kalt pilot-symol-assistert modulasjon (PSAM). Det betyr at pilot symboler (overhead informasjon) må sendes, noe som både bruker effekt og reduserer spektral effektivitet (throughput) i systemet. I denne rapporten er både piloteffekten og pilotavstanden optimalisert slik at systemets spektral effektivitet blir størst mulig, samtidig som at bitfeil raten holdes konstant. Resultater viser at effektive og pålitelige adaptive systemer kan oppnås over et stort variasjonsområde av kanalkvaliteten.

I tillegg til scenarier hvor antennene er ukorrelerte blir korrelasjon mellom antennene tatt i betraktning i et SIMO (single-input multiple-output) system. Denne gangen er estimeringen antatt som perfekt mens vi fortsatt har prediksjonsfeil. Først analyseres hvordan romlig korrelasjon påvirker throughput-raten i et system som opprinnelig er designet for å operere på ukorrelerte antenner. Deretter blir korrelasjonen tatt med i beregningen når en joint “space-time prediktor” utvikles. Som forventet er throughput-raten fortsatt lavere enn i det ukorrelerte systemet, men degradasjonen er blitt redusert. Det vil si at degradasjonen kan bli redusert når romlig korrelasjon blir utnyttet.

English summary

The focus in this report is to analyze and optimize single-carrier adaptive coded modulation systems with antenna diversity. Multidimensional trellis codes are used as component codes.

The majority of the analysis is done with both estimation and prediction errors being incorporated. Both channel estimation and prediction are performed using a pilot-symbol-assisted modulation (PSAM) scheme. Thus, known pilot symbols (overhead information) must be transmitted; which consumes power and also degrades system spectral efficiency. In this report, both power consumption and pilot insertion frequency are optimized such that they are kept at necessary values to maximize system throughput without sacrificing the error rate performance. The results show that efficient and reliable system performance can be achieved over a wide range of the considered average channel quality.

Besides the spatially uncorrelated antenna array, the effect of spatial correlation is also considered in the SIMO case. In this case, only prediction error is considered and channel estimation is assumed to be perfect. At first, the impact of spatial correlation in a predicted system originally designed to operate on uncorrelated channels is quantified. Then the correlation is taken into account by using a joint “space-time predictor”. As expected, the results show that the throughput is still lower than the uncorrelated system, but the degradation is decreased. Thus, by exploiting the correlation properly, the degradation can be reduced.

Contents

1 Introduction

There is no doubt that adaptive transmission will be deployed in a larger scale in emerging generations of wireless communication systems. This is due to the efficient use of the spectrum provided by the scheme. While adaptive transmission is not a new idea, the topic is considered in the PhD thesis [1] where some practical issues are taking into account. The thesis exists and is available in its complete form for those who finds it interesting, but it can be burdensome to read the whole thesis. Thus, this report is served as an extended abstract of the thesis for those who want to capture the concept and results without studying the thesis in details. We will not reproduce all the mathematical derivations in this report, since they easily can be found in the thesis. On the other hand, some of the derivations will be repeated to aid the reading of this report alone.

The report is two-fold. First, we will consider a general spatially uncorrelated multiple-input multiple-output (MIMO) diversity system. Other systems like single-input single-output (SISO), single-input multiple-output (SIMO), and multiple-input single-output (MISO) are obtainable from this model by choosing the correct combination of transmit and receive antennas. General motivations for adaptive transmissions and for the use of spatial diversity will be summarized in Section 2. The MIMO diversity system is introduced in Section 3. Furthermore, the transmit powers are defined in Section 4, followed by the estimation and prediction schemes in Section 5. Section 6 deals with bit error rate (BER) performance and optimal switching thresholds, whereas average spectral efficiency (ASE) performance is considered in Section 7. Numerical examples together with discussions of the results are given in Section 8. Then, a spatially correlated SIMO system is considered in Section 9. Finally, concluding remarks are drawn in Section 10.

2 Adaptive Wireless Communications Using Feedback

The demand for reliable high-rate data communication over wireless channels gives rise to the need for spectrally efficient transmission schemes. This is due to the fact that bandwidth is scarce, and both spectrum and power usage are strictly regulated. The basic idea of spectrally efficient transmission is to transmit many information bits per second per unit bandwidth on the average while maintaining a certain quality.

One way of realizing such spectrally efficient communication is by *adaptive transmission*. The success of such an adaptive transmission scheme is strongly dependent on the knowledge of the channel at the transmitter. Thus, one challenge is to extract the best possible estimate[1] of the channel

[1] In general, the term estimate of the channel here can be any kind of channel measurements which are used for adaptation purposes. The predicted/estimated channel gain or channel-signal-to-noise ratio (CSNR) is one possible measurement. Thus, it is noted that, we sometimes only use the term channel estimation or prediction for both estimation and prediction. Later on, in this report, we will use the channel estimates for decoding and detection while the prediction is used for system adaptation.

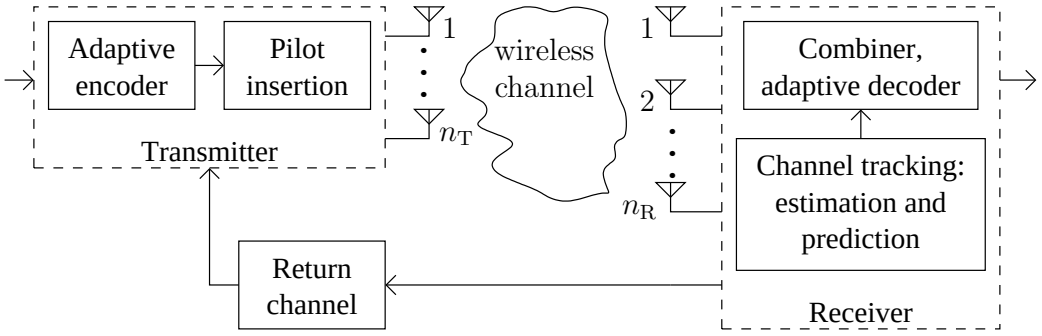

Figure 2.1: Generic figure of an adaptive coded modulation (ACM) system with multiantenna transmitter and receiver. System adaptation is based on information fed back from the receiver. Channel estimation and prediction is performed using a PSAM scheme.

at any given time. However, nature is seldom kind when it comes to wireless communications. The wireless signal, when travelling from a source to a destination, is obstructed by different objects. These objects can be small or big as e.g. leaves, trees, cars, buildings, and so on. Depending on the size of these obstacles, the signal may be reflected, scattered, and/or diffracted. Reflection of signals occurs when the signal is met by obstacles which are comparable in size to the wavelength of the signal or larger. When the obstructing object is less than the wavelength of the signal, scattering will occur. Diffraction happens when signal "bends around" obstructing objects with irregular edges [2].

A common result of these three phenomena is that the signal will arrive at the receiver from different paths and with different delays. The different replica of the signal are then summed constructively or destructively, causing fluctuation of the signal level such that the signal can be severely attenuated. This phenomenon is generally known as fading. Besides the restricted spectrum and power usage, the fading also gives rise to the need of robust and efficient transmission.

In fixed-rate and fixed-power systems, the transmission must be dimensioned relative to the worst case scenario of the channel—i.e. the system must be designed to perform acceptably in deep fades. This results in poor performance and inefficient use of spectrum when the channel condition is good. As opposed to this, spectrally efficient adaptive transmission schemes take the advantage of having a good channel by sending more bits. The rate is decreased as the channel is getting worse, and most often goes into idle when the channel is below a certain quality (then the system is said to be in outage). In order to do so, the system needs *feedback* information to assist what the transmitter should do. In order to perform such adaptations, information about the channel must be available to the transmitter and can be realized by means of a return channel (feedback channel), as shown in the generic block diagram in Figure 2.1. Here, n_{T} and n_{R} are the number of transmit and receive antennas, respectively.

The quality of the feedback information plays an important role in such an adaptive system, since it is crucial for the system to function properly. Hence, reliable estimators/predictors need to be developed and employed to reduce the effect of imperfect channel state information (CSI). However,

another approach to get around this is by more carefully designing the adaptive transmitters and receivers which account for CSI errors explicitly. This is the choice in this report.

The information about the channel is conveyed by estimating/predicting the channel variations which can be done using either non-data-aided (NDA) or data-aided (DA) schemes [3]. While NDA channel tracking schemes perform their task based on previous correctly detected symbols, the DA scheme is based on training (pilot) symbols known to both transmitter and receiver, and which are sent regularly along with the information. How often they are transmitted is dependent on the rate of time-variance of the channel. Comparing to the NDA schemes, the training-based systems must transmit overhead information which degrades the system's throughput. However, the channel can be better tracked with DA methods when the channel is fast varying or undergoes deep fades, during which the symbols are most likely to be wrongly detected so that NDA channel tracking becomes unreliable.

2.1 Effects of Space Diversity and Diversity Combining

The key concept of diversity in general is to create a number of more or less independent transmission "paths", all carrying the *same* information. In such a scenario, different signal paths may undergo independent channel fadings, leading to independent fading statistics. Thus, the probability of having all of them in a deep fade simultaneously is small. Various types of diversity techniques together with different basic combining schemes are described in [4]. In this report, we will only consider space (antenna) diversity and, hence, other techniques will not be mentioned.

Diversity combining is different from another popular and important antenna processing technique, beamforming, where the phase of signals from different antenna elements are adjusted to point a beam in a desired direction. In the diversity combining technique, the signals are combined to increase the output signal level without affecting the individual antenna pattern. On the other hand, the beamforming technique exploits the differential phase between different antennas to modify the antenna pattern of the whole array. In that way, the whole array will have a single antenna pattern once they are combined [5]. Beamforming is analyzed in e.g. [6, 7, 8, 9, 10] and is beyond of the scope of this report.

It is well known that space diversity effectively averages out deep fades and mitigates considerably the effects of imperfect channel prediction/estimation which, again, helps in improving system performance. This motivates the use of multiple-antenna reception at the receiver. In this case, we have a SIMO system. In addition, we may use multiple antennas to transmit the *same* data. In combination with multi reception we then have a MIMO diversity system, where space-time coding must be used to exploit and to achieve the available spatial diversity at the transmitter [11, 12]. Clearly, a MISO system is a special case of a MIMO diversity system where $n_{\mathrm{T}} > 1$ and $n_{\mathrm{R}} = 1$.

3 The Spatially Uncorrelated MIMO Case

In general, MIMO systems may be divided into two categories: rate maximization schemes and diversity maximization schemes, also denoted *spatial multiplexing* (SM) systems and *MIMO diversity* systems, respectively. SM offers a linear increase in the transmission rate (or capacity) at no extra bandwidth or power expenditure. This is obtained by transmitting independent data streams from each transmit antenna, or demultiplexing a single data stream in to n_{T} substreams which subsequently are transmitted from separate transmit antennas. In a rich scattering environment, the fading gains become uncorrelated. In this case, when knowledge of the channel is available at the receiver, the composite receive signal can be separated by solving linearly independent equations. Thus, the receiver can detect the different data streams, or combine the substreams into the original stream [13].

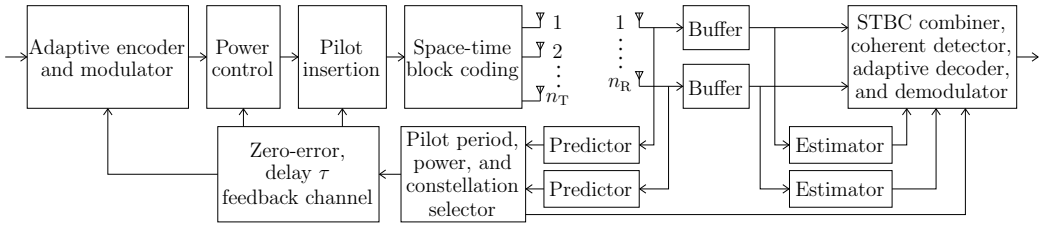

Figure 3.1: ACM system with adaptive PSAM-based channel prediction and estimation. The predicted channels are used for system adaptation and the estimated channels are used for coherent detection. The system is operating on a MIMO diversity channel.

The system under consideration is illustrated in Figure 3.1, where all subchannels between any transmitter-receiver pair are assumed to be mutually independent and Rayleigh distributed, with Jakes correlation profile.

Table 3.1: Orthogonal designs for STBC used in this chapter. Orthogonal design $\mathcal{O}_1$ and $\mathcal{O}_2$ corresponds to the regular data stream with no STBC and the Alamouti scheme, respectively. $\mathcal{O}_4$ is the orthogonal design given by in [12, matrix (40)].

Orthogonal design	n_{T}	R_s	S	T
$\mathcal{O}_1$	1	1	1	1
$\mathcal{O}_2$	2	1	2	2
$\mathcal{O}_4$	4	3/4	3	4

In order to transmit data from all of the transmit antennas simultaneously, the transmitted data must be spread both in space and time. For this operation, the space-time block codes can be used. Moreover, the orthogonal space-time block coding (STBC) is a special STBC technique designed to achieve simple decoding at the receiver. Orthogonal space-time block codes will be

Antenna no. 1	P	$\circ$	$\circ$	$\circ$	D_1	$-D_2^*$	$\frac{D_3^*}{\sqrt{2}}$	$\frac{D_3^*}{\sqrt{2}}$
Antenna no. 2	$\circ$	P	$\circ$	$\circ$	D_2	D_1^*	$\frac{D_3^*}{\sqrt{2}}$	$-\frac{D_3^*}{\sqrt{2}}$
Antenna no. 3	$\circ$	$\circ$	P	$\circ$	$\frac{D_3}{\sqrt{2}}$	$\frac{D_3}{\sqrt{2}}$	$\cdots$	$\cdots$
Antenna no. 4	$\circ$	$\circ$	$\circ$	P	$\frac{D_3}{\sqrt{2}}$	$-\frac{D_3}{\sqrt{2}}$	$\cdots$	$\cdots$

Figure 3.2: Example of a frame structure after STBC where $n_{\mathrm{T}} = 4$, and the orthogonal design $\mathcal{O}_4$ in Tab. 3.1 is used. Here, P stands for pilot and $\circ$ denotes that the system does not send anything, while Ds are data symbols. To reduce the size of the figure we avoid to write out the four last data symbols, and demonstrate only the smallest frame size.

emoployed in this report and they are listed in Tab. 3.1. These orthogonal designs and some other orthogonal designs (for both real and complex signals) can be found in [12]. The space-time encoder maps S symbols into n_{T} orthogonal sequences of length T (given as $T = (S/R_s)T_s$) where T_s is still the channel symbol interval and R_s is the rate of the employed space-time block code. The smallest frame size is illustrated in Figure 3.2. Note that the pilot symbols are not space-time block coded. Thus, the pilot is transmitted once from each antenna (time-multiplexing). While a pilot is transmitted from one antenna, the other antennas are silent such that each receiver branch can track the channel between itself and the transmitting antenna. The same pilot scheme is utilized in [14]. Note that making the pilot symbol orthogonal by spreading it with each antenna's signature code of length n_{T} does not improve the system performance since the channel predictor is found to be independent of this factor, and the mean and variance of the noise remains unchanged [15]. Also, the channel is still the same after de-spreading at the receiver.

Another possibility is to transmit sequences of orthogonal pilot symbols from different antennas (not spreading one symbol). In this case, we will need another predictor/estimator and which, we believe, is more complex than the Wiener filter in our system. This is due to the correlation properties which will be more involved since we also have to consider the intersymbol correlation within one sequence in addition to the correlation between different sequences. Moreover, the system is using the same amount of time slots also in this case [11].

4 Transmit Powers

On average, each symbol (both data and pilot symbols) is allowed to transmit with a power of $\mathcal{E}$. Thus, we need $\mathcal{E}n_{\mathrm{T}}[(L_b - n_{\mathrm{T}})R_s + 1]$ of power to transmit a whole frame. Now, we take a portion of that power (denoted by α) and allocate it to the data symbols within that frame; i.e.

$$\bar{\mathcal{E}}_d = \frac{\alpha\mathcal{E}n_{\mathrm{T}}[(L_b - n_{\mathrm{T}})R_s + 1]}{n_{\mathrm{T}}(L_b - n_{\mathrm{T}})R_s} = \frac{\alpha\mathcal{E}L}{L-1}. \tag{4.1}$$

The rest of the power is allocated to pilot symbols; i.e.

$$\mathcal{E}_{\mathrm{pl}} = (1-\alpha)\mathcal{E}L. \tag{4.2}$$

However, sometimes in ACM systems, the channel is predicted to be so bad that even the strongest code in the system's codeset can not guarrantee reliable communication. In this case, it is better not to send any data information at all. The system is said to be in outage. It means that no data power is used during the outage period. As a result, the data power can be set to

$$\mathcal{E}_d = \frac{\bar{\mathcal{E}}_d}{\text{probability of not in outage}}. \tag{4.3}$$

5 Channel Estimation and Prediction

Let $\mathbf{z}_d \in \mathbb{C}^{n_{\mathrm{R}}\times 1}$ be the received, noisy, and faded data symbol vector in complex baseband. It can be written as

$$\mathbf{z}_d(k;l) = \sqrt{\frac{\mathcal{E}_d}{n_{\mathrm{T}}}}\mathbf{H}(k;l)\mathbf{s}(k;l) + \mathbf{n}(k;l), \;\; l \in [n_{\mathrm{T}}, \cdots, L_b - 1], \tag{5.1}$$

where

$$L_b = \frac{mS}{R_s} + n_{\mathrm{T}} = \frac{L-1}{R_s} + n_{\mathrm{T}} \tag{5.2}$$

is the pilot symbol spacing *on a single antenna branch* after STBC [14] and m is a non-zero positive integer (cf. Figure 3.2 for $m = 1$). Furthermore, let $\mathbf{z}_{\mathrm{pl}} \in \mathbb{C}^{n_{\mathrm{R}}\times 1}$ be the received pilot symbol vector:

$$\mathbf{z}_{\mathrm{pl}}(k;l) = \sqrt{\frac{\mathcal{E}_{\mathrm{pl}}}{n_{\mathrm{T}}}}\mathbf{H}(k;l)\mathbf{s}(k;l) + \mathbf{n}(k;l), \;\; l \in [0, \cdots, n_{\mathrm{T}} - 1]. \tag{5.3}$$

In both equations above, the notation $x(k;l)$ is the compact way of writing $x(kL_bT_s + lT_s)$, $\mathbf{H} \in \mathbb{C}^{n_{\mathrm{R}}\times n_{\mathrm{T}}}$ is the channel gain matrix, $\mathbf{s} \in \mathbb{C}^{n_{\mathrm{T}}\times 1}$ is the vector of transmit symbols, and $\mathbf{n} \in \mathbb{C}^{n_{\mathrm{R}}\times 1}$ is the channel additive white Gaussian noise (AWGN). Without knowing the whole channel gain matrix we consider when power is equally allocated to different transmit antennas. As such, $\mathcal{E}_{\mathrm{pl}}/n_{\mathrm{T}}$ and $\mathcal{E}_d/n_{\mathrm{T}}$ is the power per pilot and per data symbol transmitted from one antenna, respectively. Moreover, we assume that $\mathsf{E}\left[|s_\mu(k;l)|^2\right] = 1$; $\mu \in [1, \cdots, n_{\mathrm{T}}]$; $l \in [n_{\mathrm{T}}, \cdots, L_b - 1]$ (data symbols), and that the pilots have unit magnitude (i.e., $|s(k;l)| = 1$ for $l \in [0, \cdots, n_{\mathrm{T}} - 1]$). Furthermore, the noise is assumed white in both space and time with zero mean and variance equal to N_0. The elements of the channel gain matrix are assumed to come from a stationary complex Gaussian RP with zero mean and unit variance.

In what follows, both the estimator and predictor are linear and made optimal in the maximum a posteriori (MAP) sense, where the temporal correlation is also assumed known. Moreover, the branches are uncorrelated by assumption and we thus can perform estimation and prediction independently on each of the receive branches.

5.1 Estimation

Based on the non-causal vector of K_e received pilot symbols $\mathbf{z}_{\mathrm{pl};\mu\nu}(k;\mu-1)$, corresponding to the pilot instances of the μ-ν antenna pair and the channel gains $\mathbf{h}_{\mathrm{pl};\mu\nu} = [h_{\mu\nu}(k-\lfloor K_e/2\rfloor;\mu-1),\cdots,h_{\mu\nu}(k+\lfloor (K_e-1)/2\rfloor;\mu-1)]^{\mathsf{T}}$, a *non-causal* MAP estimator estimates the fading channel gain in the set $\{h_{\mu\nu}(k;l)\}_{l=n_{\mathrm{T}}}^{L_b-1}$ as

$$h_{e;\mu\nu}(k;l) = \mathbf{w}_e^{\mathsf{H}}\mathbf{z}_{\mathrm{pl};\mu\nu}(k;\mu-1), \quad \text{for } \mu\in[1,\cdots,n_{\mathrm{T}}],\ \nu\in[1,\cdots,n_{\mathrm{R}}], \tag{5.4}$$

where $\mathbf{w}_e$ is the MAP-optimal estimator obtained by solving normal equations. Here, $(\cdot)^{\mathsf{T}}$ and $(\cdot)^{\mathsf{H}}$ denote transpose and complex conjugate transpose, respectively.

Assuming the same pilot is transmitted from all of the transmit antennas and defining the estimation error as $\epsilon_{e;\mu\nu}(k;l) = h_{\mu\nu}(k;l) - h_{p;\mu\nu}(k;l)$, the MMSE of any subchannel can be calculated as

$$\sigma^2_{e;\mu\nu}(l) = \mathsf{E}\big[|\epsilon_{e;\mu\nu}|^2\big] = 1 - \sum_{\kappa=1}^{K_e}\frac{|\mathbf{u}_\kappa^{\mathsf{H}}\mathbf{r}_e|^2(1-\alpha)L\bar{\gamma}_b}{(1-\alpha)L\bar{\gamma}_b\lambda_\kappa + n_{\mathrm{T}}} \tag{5.5}$$

In above equation, $\{\mathbf{u}_\kappa\}$ denotes the eigenvectors of the covariance matrix $\mathbf{R}_e = \mathsf{E}\big[\mathbf{h}_{\mathrm{pl};\mu\nu}\mathbf{h}_{\mathrm{pl};\mu\nu}^{\mathsf{H}}\big]$, $\{\lambda_\kappa\}$ are the corresponding eigenvalues, and $\mathbf{r}_e$ is the covariance vector; $\mathbf{r}_e = \mathsf{E}\big[\mathbf{h}_{\mathrm{pl};\mu\nu}h^*_{\mu\nu}(k;l)\big]$. Moreover, $\bar{\gamma}_b = \mathcal{E}/N_0$ is the expected channel-signal-to-noise ratio CSNR on *one* receive branch.[2]

5.2 Prediction

We assume that the transmitter adaptation occurs only once per transmission frame of L_b symbols. Thus, the *causal* predictor uses K_p pilot symbols from the past to predict one sample in the set $\{h_{\mu\nu}(k;l)\}_{l=n_{\mathrm{T}}}^{L_b-1}$ of the kth frame, which is $\tau = DL_bT_s$ seconds ahead in time. Here, D is the distance measured in the number of frames.

Let the channel gain vector of one subchannel (corresponding to the pilot instants vector $\mathbf{z}_{\mathrm{pl};\mu\nu}(k;\mu-1)$) used in the prediction be $\mathbf{h}_{\mathrm{pl};\mu\nu} = [h_{\mu\nu}(k-D;\mu-1),\cdots,h_{\mu\nu}(k-D-K_p+1;\mu-1)]^{\mathsf{T}}$, the covariance matrix and the covariance vector is now $\mathbf{R}_p = \mathsf{E}\big[\mathbf{h}_{\mathrm{pl};\mu\nu}\mathbf{h}_{\mathrm{pl};\mu\nu}^{\mathsf{H}}\big]$ and $\mathbf{r}_p = \mathsf{E}\big[\mathbf{h}_{\mathrm{pl};\mu\nu}h^*_{\mu\nu}(k;l)\big]$, respectively. Similar to the estimation case, the predicted channel is a linear combination of the received pilot symbols; denoted by $h_{p;\mu\nu}(k;l) = \mathbf{w}_p^{\mathsf{H}}\mathbf{y}_{\mathrm{pl};\mu\nu}(k;\mu-1)$. Let $\epsilon_{p;\mu\nu}(k;l) = h_{\mu\nu}(k;l) - h_{p;\mu\nu}(k;l)$ and given the predictor $\mathbf{w}_p$—which can be obtained similarly to the estimation case—the MMSE of the prediction error is

$$\sigma^2_{p;\mu\nu}(l) = \mathsf{E}\big[|\epsilon_{p;\mu\nu}|^2\big] = 1 - \sum_{\kappa=1}^{K_p}\frac{|\mathbf{u}_\kappa^{\mathsf{H}}\mathbf{r}_e|^2(1-\alpha)L\bar{\gamma}_b}{(1-\alpha)L\bar{\gamma}_b\lambda_\kappa + n_{\mathrm{T}}}, \tag{5.6}$$

where $\{\mathbf{u}_\kappa\}$ and $\{\lambda_\kappa\}$ are now the sets of eigenvectors and eigenvalues of $\mathbf{R}_p$, respectively.

[2] Which is the sum of all the subchannels' average CSNR received in one antenna. That is: $\bar{\gamma}_b = \sum_{a=1}^{n_{\mathrm{T}}}\bar{\gamma}_{ab} = \sum_{a=1}^{n_{\mathrm{T}}}\mathcal{E}/(n_{\mathrm{T}}N_0) = \mathcal{E}/N_0$.

Due to the assumption of independent branches, both estimation MMSE and prediction MMSE are the same on all branches. That is,

$$\sigma^2_{e;\mu\nu}(l) = \sigma^2_e(l), \tag{5.7a}$$

$$\sigma^2_{p;\mu\nu}(l) = \sigma^2_p(l) \tag{5.7b}$$

$\forall\ \mu \in [1, \cdots, n_{\mathrm{T}}]$ and $\nu \in [1, \cdots, n_{\mathrm{R}}]$.

6 BER Performance and Optimal Switching Thresholds

In this report, the ACM system is using a set of eight 4-dimensional (4-D) trellis codes as component codes to switch between. The exact BER performance of these codes can not be found, but it can be approximated by

$$\mathrm{BER}(M_n|\gamma) = \sum_{\ell=1}^{\mathcal{L}} a_n(\ell) \exp\left(-\gamma \frac{b_n(\ell)}{M_n}\right). \tag{6.1}$$

Here γ is the instantaneous CSNR and $\mathcal{L}$ is the number of exponential functions which approximate the simulated BER (we use $\mathcal{L} = 3$). Moreover $a_n(\ell)$ and $b_n(\ell)$ are constellation dependent constants obtained by first simulating the codes' BER performance on AWGN channels and then using curve fitting with the least square method. These constants are given in Tab. 6.1 and the approximation is illustrated in Figure 6.1 for different constellation sizes. At first sight, the approximation seems to be quite coarse. However, it is shown in [1] that the ACM performance results of this approximation are very close to those obtained when the tight approximation of [16] is used.

Table 6.1: The code-dependent constants $\{a_n(\ell)\}_{\ell=1}^3$ and $\{b_n(\ell)\}_{\ell=1}^3$ for the example 4-D trellis codes.

n	$a_n(1)$	$b_n(1)$	$a_n(2)$	$b_n(2)$	$a_n(3)$	$b_n(3)$
1	233.8034	12.4335	-280.8712	11.4405	51.3394	8.6131
2	210.6415	8.4208	-242.0657	7.9916	34.3732	6.0432
3	246.0565	7.7677	-334.6900	8.1130	89.4924	9.1087
4	99.7887	7.7426	-160.6040	8.3843	61.5091	9.4667
5	78.0083	7.0135	-100.8414	7.4793	23.4319	9.0714
6	86.2181	7.3704	-96.0270	7.6780	10.3583	10.3191
7	87.6912	7.0471	-94.5020	7.2852	7.3344	10.1898
8	89.3099	7.2848	-95.6889	7.4987	6.8972	10.4428

Based on the matrix of the estimated channel gains $\mathbf{H}_e$, the signal is space-time combined and decoded at the receiver [11]. Although the result of the space-time combining scheme is different

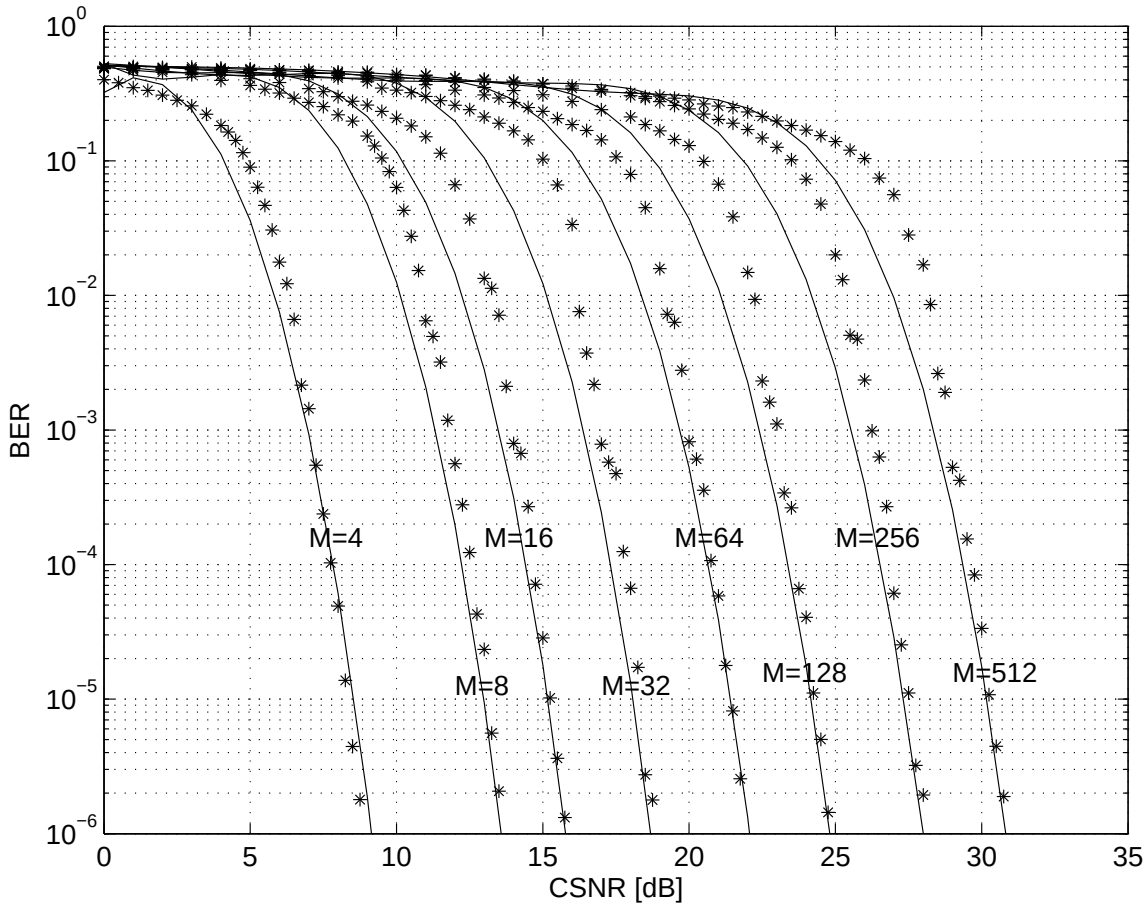

Figure 6.1: BER performance of trellis codes on AWGN channels for different M-QAM constellations. The solid lines denote the approximations, while the stars represent the simulated values.

from the traditional MRC, the resulting effective CSNR is still the same. The difference of these two combining techniques is a complex conjugation of the noise which appears in the space-time combining scheme. This conjugation does not play any role when we take the absolute value; which is exactly what we do when we calculate the CSNR. Thus, the total CSNR still can be found by using the MRC approach, which is the sum of the subchannels' CSNR. Hence, the BER of (6.1) now becomes

$$\text{BER}\left(M_n \middle| \{h_{e;\mu\nu}\}\right) = \sum_{\ell=1}^{\mathcal{L}} a_n(\ell) \exp\left(-A_n(\ell)\mathcal{E}_d \|\mathbf{H}_e\|_{\mathsf{F}}^2\right), \tag{6.2}$$

where $A_n(\ell) = b_n(\ell)/[n_{\mathrm{T}} M_n(N_0 + g\mathcal{E}_d\sigma_e^2(l))]$ and $\|\cdot\|_{\mathsf{F}}$ is the Frobenious norm.

With the assumption that the subchannels are independent, the overall conditional PDF of the set $\{|h_{e;\mu\nu}|\}$ given the set $\{h_{p;\mu\nu}\}$ is a product of the conditional PDF of each subbranch. That is

$$f_{h_e|h_p}\left(\{|h_{e;\mu\nu}|\} \,\middle|\, \{h_{p;\mu\nu}\}\right) = \prod_{\mu=1}^{n_{\mathrm{T}}} \prod_{\nu=1}^{n_{\mathrm{R}}} f_{h_{e;\mu}|h_{p;\mu}}\left(|h_{e;\mu\nu}| \middle| h_{p;\mu\nu}\right).$$

Each subchannel is Rician distributed with the Rice factor $K = |h_{p;\mu\nu}(k;l)|^2/\sigma^2_{h_{e;\mu\nu}|h_{p;\mu\nu}}$. Invoking

the assumption in (5.7), the Rician factor of each subchannel simplifies to $K = |h_{p;\mu\nu}(k;l)|^2/\sigma^2_{h_e|h_p}$ where, by assumption, $\sigma^2_{h_{e;\mu\nu}|h_{p;\mu\nu}} = \sigma^2_p - \sigma^2_e = \sigma^2_{h_e|h_p}\ \forall \mu,\nu$.

The BER conditioned on the set of predicted channels is obtained by averaging (6.2) over the product of the Rician PDFs:

$$\begin{aligned}\mathrm{BER}\left(M_n\middle|\,\{h_{p;\mu\nu}\}\right) &= \underbrace{\int_0^\infty \cdots \int_0^\infty}_{n_\mathrm{T}n_\mathrm{R}-\text{fold}} \mathrm{BER}\left(M_n\middle|\,\{|h_{e;\mu\nu}|\}\right) \\ &\quad \times f_{h_e|h_p}\left(\{|h_{e;\mu\nu}|\}\,\middle|\,\{h_{p;\mu\nu}\}\right) d|h_{e;1,1}|\cdots d|h_{e;n_\mathrm{T},n_\mathrm{R}}| \\ &= \sum_{\ell=1}^{\mathcal{L}} a_n(\ell) d_n(\ell)^{n_\mathrm{T}n_\mathrm{R}} \exp\!\left(-A_n(\ell)d_n(\ell)\mathcal{E}_d\|\mathbf{H}_p\|_\mathsf{F}^2\right), \end{aligned} \tag{6.3}$$

after some straightforward integrations (with the help of [17, Eq. (6.633-4)]) where, for notational brevity, $d_n(\ell) = 1/(A_n(\ell)\mathcal{E}_d\sigma^2_{h_e|h_p} + 1)$.

Let $\mathbf{H}_p = \mathbf{H} - \mathbf{\Xi}_p$ be the matrix containing the predicted channels and let $\mathbf{\Xi}_p$ be the matrix of the corresponding prediction errors with the elements $[\mathbf{\Xi}_p]_{\nu\mu} = \epsilon_{p;\mu\nu}$. The total predicted CSNR per symbol can be written as

$$\hat{\gamma} = \frac{\bar{\mathcal{E}}_d\|\mathbf{H}_p\|_\mathsf{F}^2}{n_\mathrm{T}N_0} = \frac{\bar{\gamma}_b\bar{\mathcal{E}}_d\|\mathbf{H}_p\|_\mathsf{F}^2}{n_\mathrm{T}\mathcal{E}}. \tag{6.4}$$

Solving it with respect to $\|\mathbf{H}_p\|_\mathsf{F}^2$ and inserting the solution into (6.3) gives

$$\mathrm{BER}(M_n|\hat{\gamma}) = \sum_{\ell=1}^{\mathcal{L}} a_n(\ell) d_n(\ell)^{n_\mathrm{T}n_\mathrm{R}} \exp\!\left(-\frac{\hat{\gamma}A_n(\ell)d_n(\ell)n_\mathrm{T}\mathcal{E}\mathcal{E}_d}{\bar{\gamma}_b\bar{\mathcal{E}}_d}\right), \tag{6.5}$$

and the optimal switching thresholds $\{\hat{\gamma}\}_{n=1}^N$ are subsequently found by solving $\mathrm{BER}(M_n|\hat{\gamma}) = \mathrm{BER}_0$. Obviously, a numerical approach must be use to find the solutions.

From (6.4) the average predicted CSNR is

$$\bar{\hat{\gamma}} = \frac{\bar{\mathcal{E}}_d\mathsf{E}\left[\|\mathbf{H}_p\|_\mathsf{F}^2\right]}{n_\mathrm{T}N_0} = \frac{r\bar{\gamma}_b n_\mathrm{T}n_\mathrm{R}}{n_\mathrm{T}} \tag{6.6}$$

where $r = \bar{\mathcal{E}}_d(1-\sigma_p^2)/\mathcal{E}$, and the total predicted CSNR follows the gamma distribution with the mean given in (6.6) [14, 18]. That is: $\hat{\gamma} \sim \mathcal{G}\left(n_\mathrm{T}n_\mathrm{R}, r\bar{\gamma}_b/n_\mathrm{T}\right)$.

The average BER is defined as the ratio between the number of bits received in error, and the number of bits transmitted in total:

$$\overline{\mathrm{BER}} = \frac{\sum_{n=1}^N \mathrm{BER}(M_n)\cdot R_n^{\mathrm{STBC}}}{\sum_{n=1}^N P_n \cdot R_n^{\mathrm{STBC}}}, \tag{6.7}$$

where R_n^{STBC} is the spectral efficiency (SE) of the nth constellation after STBC (to be derived in

Section 7),

$$\begin{aligned}\mathrm{BER}(M_n) &= \int_{\hat{\gamma}_n}^{\hat{\gamma}_{n+1}} \mathrm{BER}(M_n|\hat{\gamma}) f_{\hat{\gamma}}(\hat{\gamma}) d\hat{\gamma} \\ &= \sum_{\ell=1}^{\mathcal{L}} a_n(\ell) \left(\frac{d_n(\ell)\bar{\mathcal{E}}_d}{r d_n(\ell) A_n(\ell) \mathcal{E}\mathcal{E}_d + \bar{\mathcal{E}}_d} \right)^{n_\mathrm{T} n_\mathrm{R}} \\ &\quad \times \left\{ \overline{\Gamma}\left(n_\mathrm{T} n_\mathrm{R}, n_\mathrm{T} \hat{\gamma}_n \frac{r d_n(\ell) A_n(\ell) \mathcal{E}\mathcal{E}_d + \bar{\mathcal{E}}_d}{r \bar{\gamma}_b \bar{\mathcal{E}}_d} \right) \right. \\ &\quad \left. - \overline{\Gamma}\left(n_\mathrm{T} n_\mathrm{R}, n_\mathrm{T} \hat{\gamma}_{n+1} \frac{r d_n(\ell) A_n(\ell) \mathcal{E}\mathcal{E}_d + \bar{\mathcal{E}}_d}{r \bar{\gamma}_b \bar{\mathcal{E}}_d} \right) \right\}, \end{aligned} \tag{6.8}$$

and P_n is the probability that $\hat{\gamma} \in [\hat{\gamma}_n, \hat{\gamma}_{n+1}\rangle$:

$$P_n = \int_{\hat{\gamma}_n}^{\hat{\gamma}_{n+1}} f_{\hat{\gamma}}(\hat{\gamma}) d\hat{\gamma} = \overline{\Gamma}\left(n_\mathrm{T} n_\mathrm{R}, \frac{n_\mathrm{T} \hat{\gamma}_n}{r \bar{\gamma}_b} \right) - \overline{\Gamma}\left(n_\mathrm{T} n_\mathrm{R}, \frac{n_\mathrm{T} \hat{\gamma}_{n+1}}{r \bar{\gamma}_b} \right). \tag{6.9}$$

Here, $\overline{\Gamma}(a, x) = \Gamma(a, x)/\Gamma(a)$ is the normalized incomplete gamma function.

7 Optimization of ASE

The SE of the nth constellation used by a 4-D trellis code with a PSAM scheme is $R_n = (1 - 1/L)(\log_2(M_n) - 1/2)$. After STBC using the orthogonal designs in Tab. 3.1, the effective SE becomes

$$\begin{aligned} R_n^{\mathrm{STBC}} &\overset{(a)}{=} \left(\log_2(M_n) - \frac{1}{2} \right) \frac{L_b - n_\mathrm{T}}{L_b} R_s \\ &= \left(\log_2(M_n) - \frac{1}{2} \right) \frac{(L-1) R_s}{L - 1 + n_\mathrm{T} R_s}. \end{aligned} \tag{7.1}$$

The term outside of the parenthesis in the equality marked with (a) corresponds to the fact that if the frame length L_b is equal to n_T, then no data information is transmitted. Thus, the SE must be zero. Using orthogonal STBC, there is a rate penalty for complex signals when $n_\mathrm{T} > 2$. That explains the rate R_s in the above expressions. The second equality is obtained by using $L_b = (L-1)/R_s + n_\mathrm{T}$ (introduced in Eq. (5.2)).

Hence, the overall ASE is given by

$$\mathrm{ASE} = \sum_{n=1}^{N} R_n^{\mathrm{STBC}} \cdot P_n. \tag{7.2}$$

Before invoking the optimization algorithm to do the maximization, the following choices are made. It is obvious that the variance of the *prediction* error is largest when predicting the last symbol in a frame ($l = L_b - 1$). As a result, prediction of the symbol located at the end of the frame based on the pilots transmitted from, e.g., the fourth antenna is slightly more accurate than it would be if based on pilots from the first antenna (cf. Figure 3.2). On the other hand, the variance of the

estimation error is almost the same for all l, if the order of the estimator is $K_e \geq 20$ [19]. Thus, we use the *estimation* error variance $\sigma_e^2 = \sigma_{e;\mu\nu}^2(L_b - 1)$, and the conservative choice of the *prediction* error variance $\sigma_p^2 = \sigma_{p;1\nu}^2(L_b - 1)$—note the subscript index—when finding the optimal switching thresholds $\{\hat{\gamma}_n\}_{n=1}^N$, as well as in the further optimization process.

When using Nyquist sampling, L must be less than $L_{\max} = \lfloor 1/(2f_dT_s) \rfloor$ [20] where f_d is the maximum Doppler shift. Thus, for $L \in [2, \cdots, L_{\max}]$ we have the following optimization problem:

$$\begin{aligned} &\max_{\alpha} \ \text{ASE} \\ &\text{subject to } \ 0 < \alpha < 1. \end{aligned} \tag{7.3}$$

Clearly, numerical optimization must be used in this case. For this purpose we have used the function `fminbnd` in MATLAB.

After solving (7.3) for all the possible L values, the maximum ASE is found by searching over all L in order to find the α and the L values which simultaneously maximize ASE.

8 Numerical Example and Discussion

At this point, we consider an example ACM system which has a set of $N = 8$ QAM signal constellations of sizes $\{M_n\} = \{4, 8, 16, 32, 64, 128, 256, 512\}$ to switch between. These constellations are used to code and decode eight 4-dimensional trellis codes [16]. We assume that the expected subchannel CSNR is the same for all the branches. The carrier frequency is $f_c = 2$ GHz and the length of a channel symbol is $T_s = 5$ μs—corresponding to a channel bandwidth of 200 kHz using Nyquist sampling. With the mobile velocity $v = 30$ m/s and the given carrier frequency, the Doppler frequency is $f_d = 200$ Hz. We require the system to tolerate a $\text{BER}_0 = 10^{-5}$, and we choose the order of the estimator and predictor to be $K_e = 20$ and $K_p = 250$, respectively. This choice of K_p leads to a suboptimal but satisfactory predictor [21].

The system delay considered is $\tau = DL_bT_s = 1$ ms (corresponding to the normalized delay $f_d\tau = 0.2$). Applying (5.2) the following results are obtained:

- $n_{\text{T}} = 1$: $L = L_b \in \{2, 4, 5, 8, 10, 20, 25, 40, 50, 100, 200\}$.
- $n_{\text{T}} = 2$: $L_b \in \{4, 8, 10, 20, 40, 50, 100, 200\}$.
  Thus, $L \in \{3, 7, 9, 19, 39, 49, 99, 199\}$.
- $n_{\text{T}} = 4$: $L_b \in \{8, 20, 40, 100, 200\}$.
  Thus, $L \in \{4, 13, 28, 73, 148\}$.

It is noted that when both $n_{\text{T}} = 1$ and $n_{\text{R}} = 1$, the analysis in this chapter reduces to the SISO case. The uncorrelated SIMO system is obtained if $n_{\text{T}} = 1$ and $n_{\text{R}} > 1$. Furthermore, when $n_{\text{T}} > 1$ and $n_{\text{R}} = 1$ we have a MISO system.

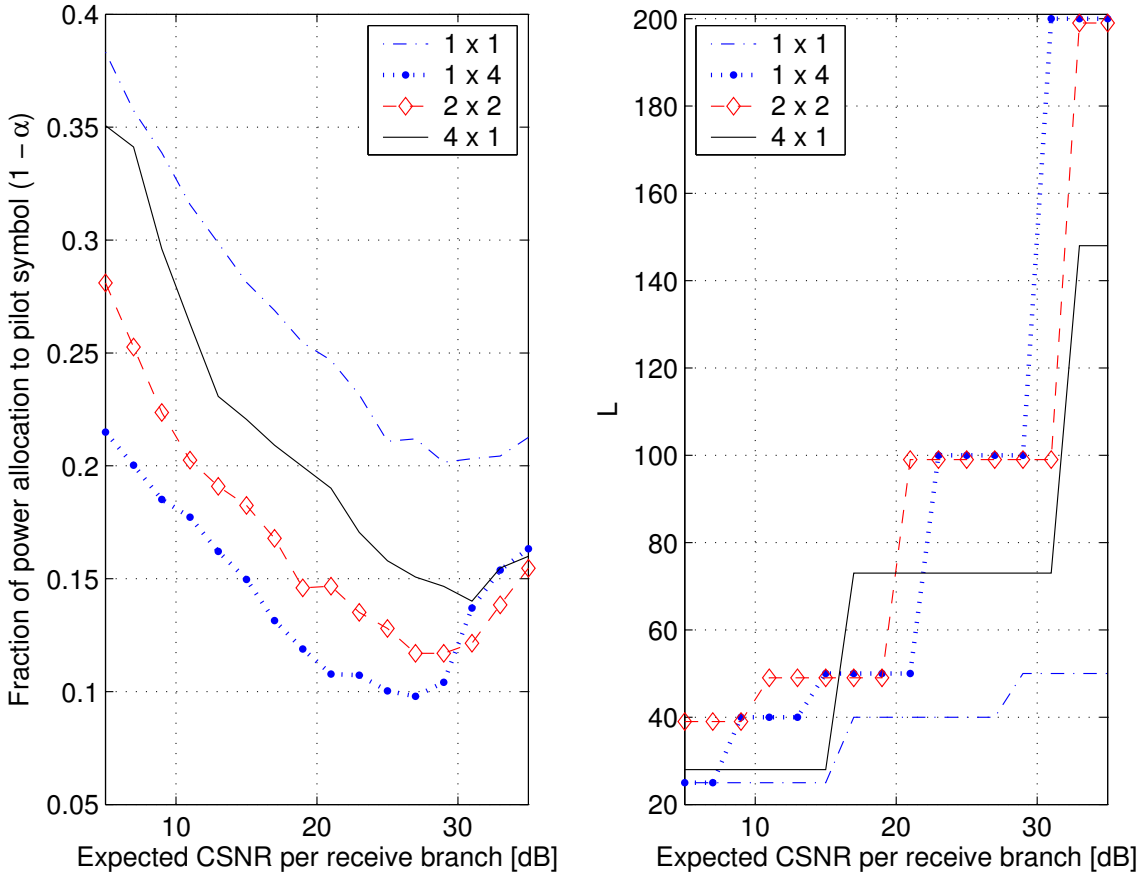

Figure 8.1: **Left panel:** *Optimal fraction of power allocated to pilot symbols (i.e.* $1-\alpha$*) when the pilot period* L *is optimal.* **Right panel:** *Optimum pilot spacing* L *when the power is optimally allocated between pilot and data symbols. Both figures are generated for different combinations of transmit and receive antennas.*

How power is optimally allocated to pilot symbols and how the optimal pilot symbol spacing L is distributed with the average CSNR can be read from Figure 8.1. The amount of power allocated to data symbols is also easily read from that figure. Clearly, the pilot period L increases with increasing CSNR and it increases faster with higher diversity order. Moreover, it is apparent that, in most of the CSNR region, necessary pilot power decreases with increasing average CSNR—i.e. more power should be put on data symbols when the average CSNR is increased. The more antennas there are—either on the transmitter side or on the receiver side, or on both sides—the less power is allocated to pilot symbols. This is also to be expected since the antennas in this particular system are used to increase the diversity order, i.e. to stabilize the channel.

For the same diversity order (the product $n_{\mathrm{T}} \times n_{\mathrm{R}}$), most of the power is left for data symbols in the SIMO case. Having higher *transmit* diversity, the pilot power *on each antenna* is reduced when the average total transmit power $\mathcal{E}$ is fixed. Thus, if the pilots are to "survive" after the transmission over the individual channels, more *total* power must be assigned on them. That is the case for $n_{\mathrm{T}} = 4$

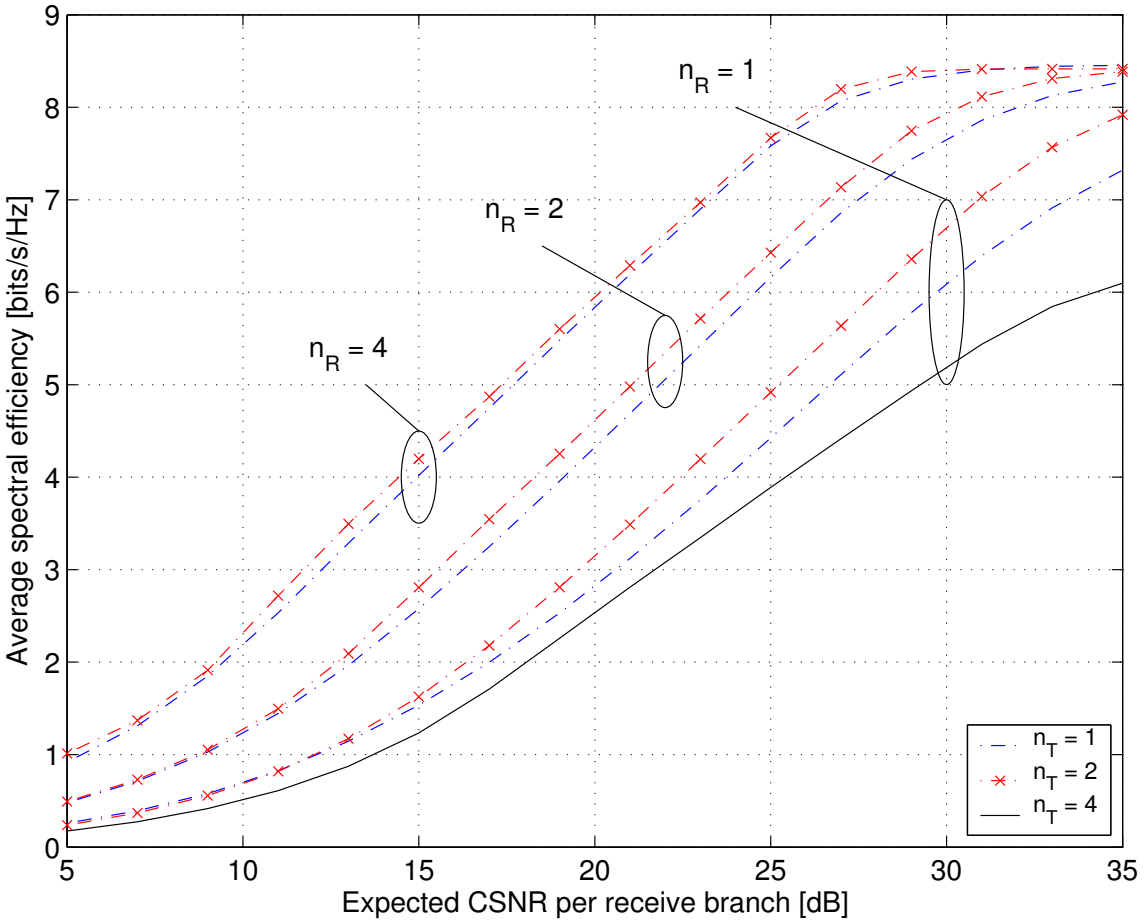

Figure 8.2: Average spectral efficiency for different combinations of transmit and receive antennas ($n_{\mathrm{T}} \times n_{\mathrm{R}}$): ($1 \times 1$), ($1 \times 2$), ($1 \times 4$), ($2 \times 1$), ($2 \times 2$), ($2 \times 4$), and ($4 \times 1$), respectively. The curves are generated when both power distribution between pilot and data symbol and pilot spacing are optimal.

in the left panel of Figure 8.1. Seeing this together with the ASE performance in Figure 8.2, from an ASE point of view the SIMO solution is clearly preferred to other combinations of transmit and receive antennas yielding the *same diversity order*.

In [14], the ASE was always reduced when having two transmit antennas compared to when only one transmit antenna is employed. In contrast to this, Figure 8.2 shows that the ASE is increased by going from 1 transmit antenna to 2 transmit antennas, as long as the pilot spacing and the power distribution are optimal. In general, when using STBC, the channel capacity is reduced, except when the rate of the employed space-time block code is one and the channel is rank one [22]. In our example, only the orthogonal design $\mathcal{O}_2$ for $n_{\mathrm{T}} = 2$ has rate one (no STBC is necessary for $n_{\mathrm{T}} = 1$). Optimization of the system with 2 transmit antennas also gives a larger pilot spacing and a lower pilot power. As a result, in this case, the ASE becomes higher compared to the system with only one transmit antenna. This result agrees well with [23].

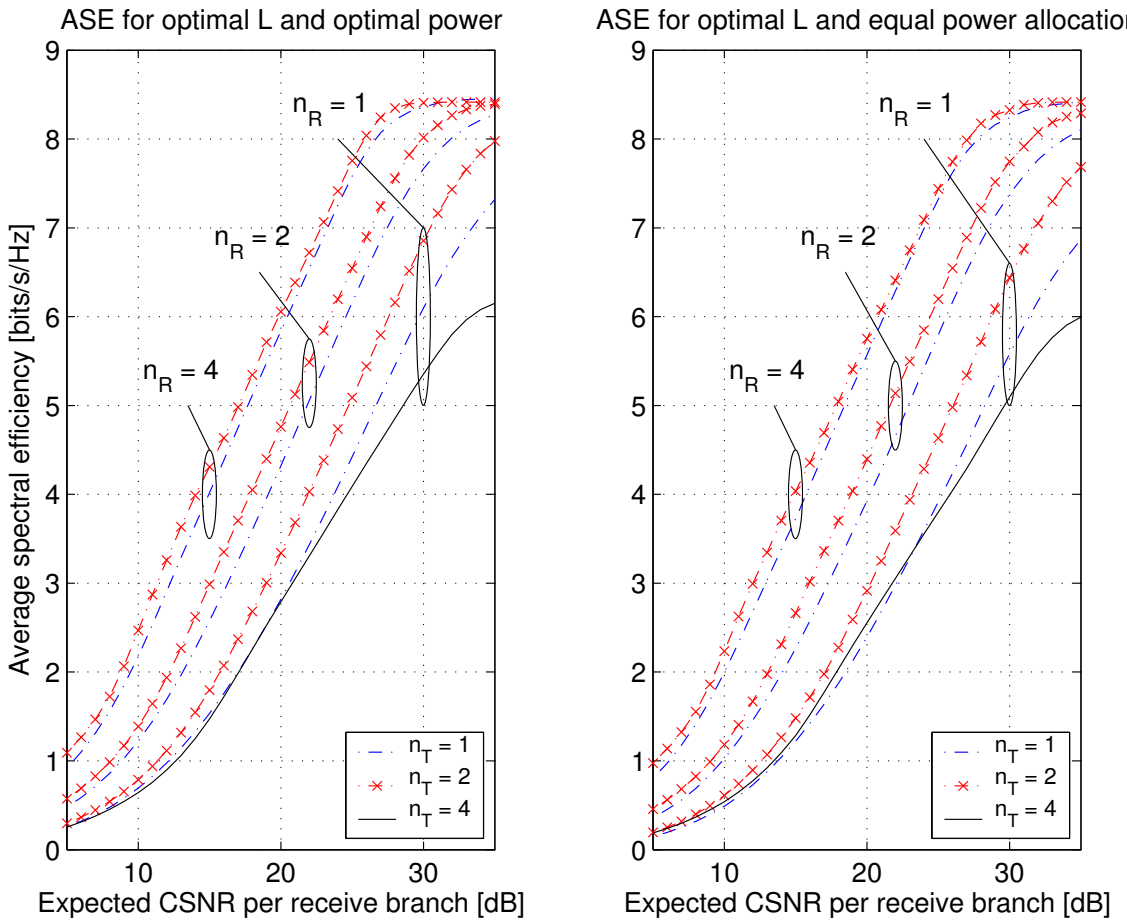

Figure 8.3: Comparison of ASE when both power allocation and pilot spacing are optimal (left panel) with optimal pilot spacing and equal power allocation (right panel).

For comparison purposes, we include two plots of ASE corresponding to 1) optimal power and optimal pilot period, and 2) equal power allocation and optimal pilot period. They are depicted on the left and right panel of Figure 8.3, respectively. Also, here, the gain by having optimal L and α (optimal power distribution) is larger. The gain is up to approximately 0.5 bits/s/Hz.

When we have 4 transmit antennas, the employed space-time block code only has rate 3/4; hence, some symbols must be transmitted several times, and the throughput is significantly reduced due to that loss. When performing channel estimation and prediction using PSAM in a MIMO diversity system with n_{T} transmit antennas, the overall number of pilot symbols to be transmitted is n_{T} times the number of pilot symbols that are needed in the non-MIMO case [11] (either by using orthogonal pilot symbols, or the pilots must be transmitted one at a time from each antenna). Moreover, using the pilot transmission scheme in this paper (or spreading one pilot symbol as in [15]) the system is losing $n_{\mathrm{T}}(n_{\mathrm{T}}-1)$ symbol intervals where data symbols could be transmitted such that the system performance could be increased.

The $\overline{\mathrm{BER}}$ performance is shown in Figure 8.4. As observed, our requirement of $\mathrm{BER}_0 = 10^{-5}$ is

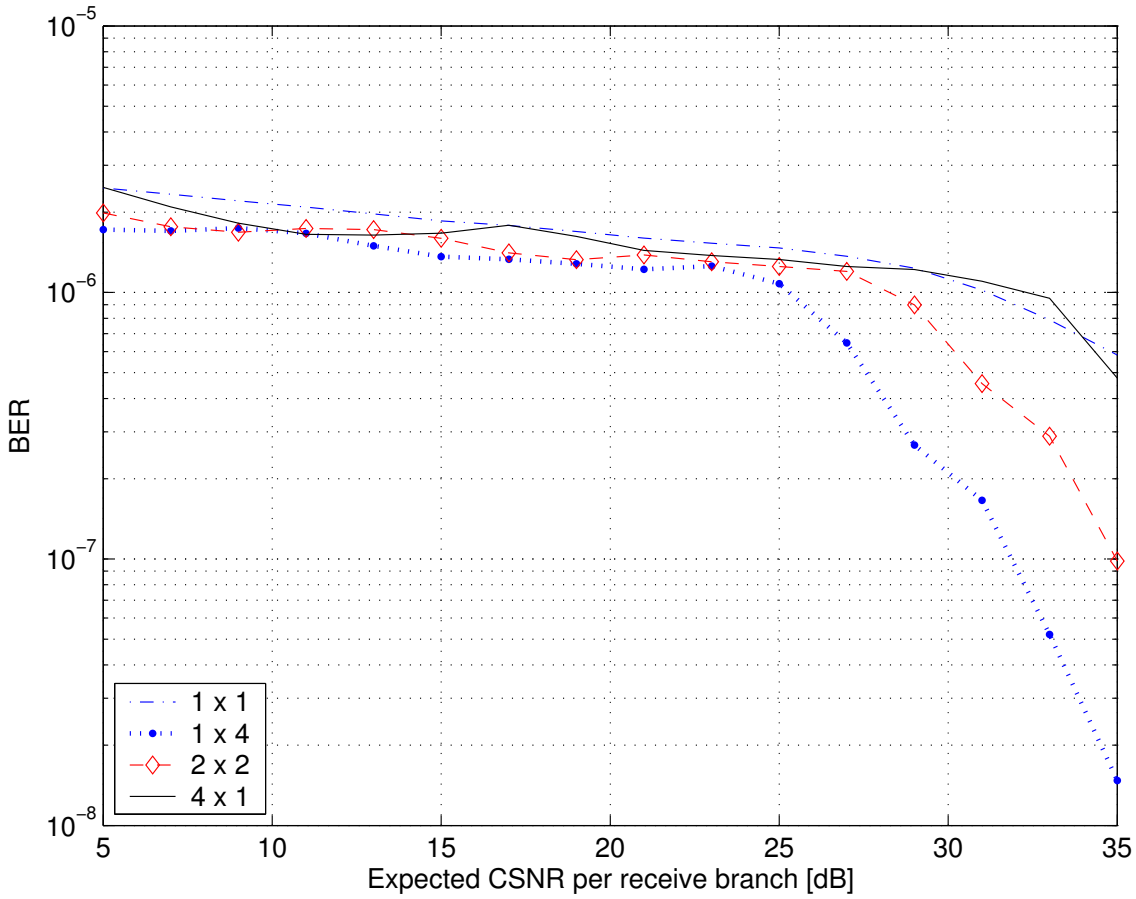

Figure 8.4: Average BER when the power and the pilot spacing are optimal for different combinations of transmit and receive antennas.

always satisfied since we require the *instantaneous* BER of the system to be always below BER_0. On the other hand, the curves are unnecessarily far below the requirement. To reduce that gap, we can modify the constraint in such a way that the *average* BER (instead of the instantaneous BER) must be lower than BER_0. In that way, the throughput increases and the system becomes less sensitive to the time delay, as [24] concluded. Optimization of switching thresholds with respect to average BER constraint is also analyzed in [25], [26, Chap. 12]]. Figure 8.4 also confirms the fact that orthogonal STBC gives full spatial diversity order (the product $n_\mathrm{T} \times n_\mathrm{R}$) by looking at the slope of the $\overline{\mathrm{BER}}$ curves at high CSNR.

9 Impact of Spatial Correlation

In order to have uncorrelated subchannels, the receive antennas must be spaced at least half a wavelength apart [2]. However, from an experimental point of view, about 10–20 wavelengths separation between the antenna elements is sometimes required to provide sufficient spatial decorrelation at the

outdoor base station [27]. Similarly, sufficient spatial decorrelation between the receive antennas at the MS or between the antennas of an indoor BS is obtained by separating the antennas by quarter of a wavelength [27].

Due to physical size limitations, the antennas might however be spaced quite close to each other. This implies that there exists some correlation between these antennas. Insufficient scattering around the base station also leads to correlated branches [13]. In such a system, spatial correlation is playing an important role when analyzing the system performance, since it is well known that correlation degrades performance [28]. However, this degradation can be reduced if the correlation is exploited properly.

In this section, we consider a SIMO system and we assume that the channel estimation is perfect and that branches are identically distributed but spatially correlated. The correlation between two antennas reduces exponentially with the distance between them. Only numerical results are given here, whereas the analysis can be carried out similarly to the spatially uncorrelated case and the analytical expressions can be found in the thesis. Of course, there are differences in the analysis, but the main difference here compared to the previous sections is the fact that the PDF of the combined CSNR is no longer a gamma distribution. However, in order to model the joint PDF of true and predicted CSNRs we approximate the marginal PDFs to be a gamma distribution with the two first moments equal to the exact PDF. We also assume that the space-time correlation function is separable, meaning that it can be represented as a product of spatial and temporal correlation functions.

We see from Figure 9.1 that ASE is reduced with increased spatial correlation between the antennas. This is in principle expected, since the advantages of having antenna diversity become smaller with larger spatial correlation. It should be noted that the subchannels are predicted independently of each other where the spatial correlation is not taken into account. This is clearly not optimal, but it gives the expected performance when the spatial correlation is not known or not exploited. The exploitation of the spatial correaltion is considered next.

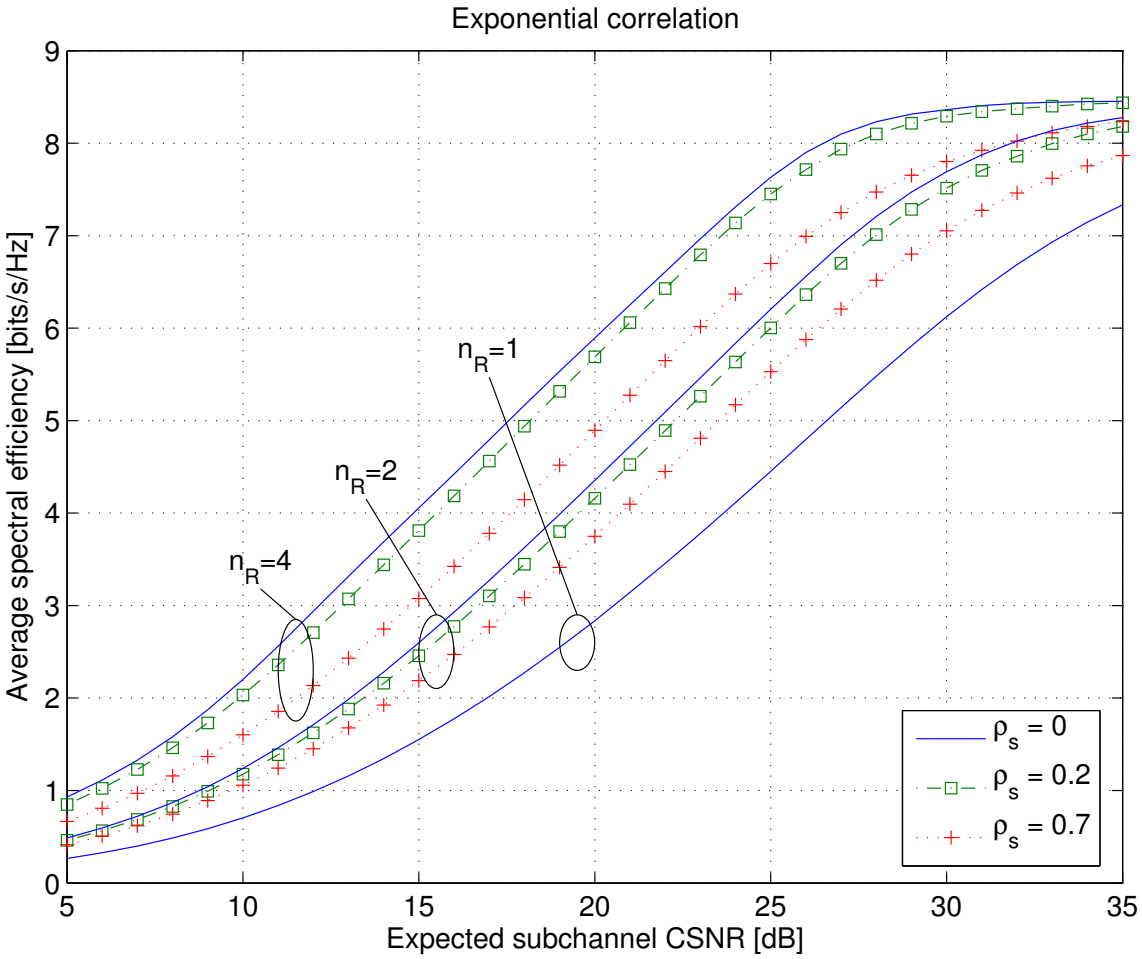

Figure 9.1: ASE as a function of subchannel CSNR for optimal L and optimal power allocation. The correlation between the subchannels is decreasing with the distance between them (exponential correlation model) and is equal to $\rho_s = 0$, 0.2, and 0.7, respectively.

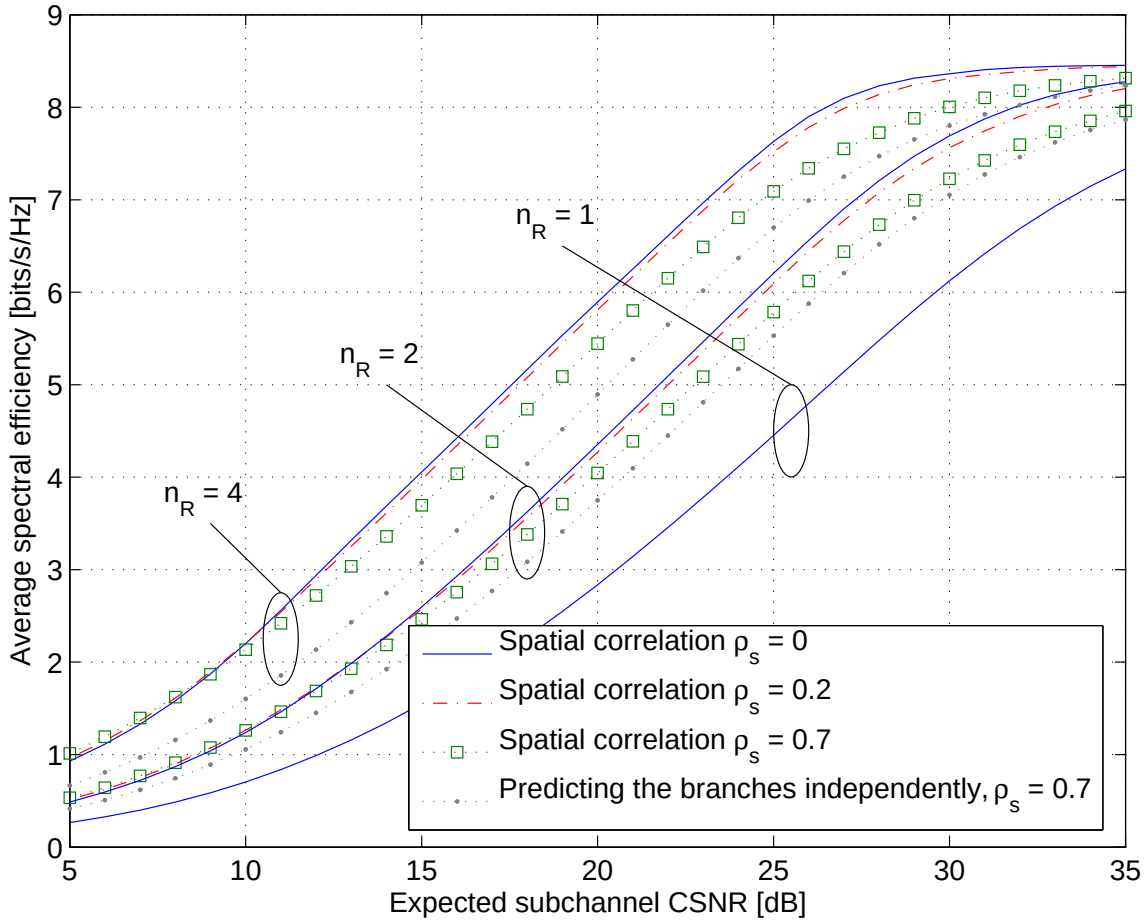

Figure 9.2: Average spectral efficiency as a function of expected CSNR on one branch for different combinations of number of antennas and spatial correlations. It is also plotted for when the subchannels are predicted independently for $\rho_s = 0.7$.

In Figure 9.2, we assume that the spatial correlation is known so that it can be taken into account. Thus, a "space-time predictor" is needed and must be derived. It is clear that the loss in ASE due to spatial correlation is reduced when all subchannels are *jointly* predicted. The gain is larger when there are many antennas available to combine. However, and as expected, the ASE is still smaller than the uncorrelated case.

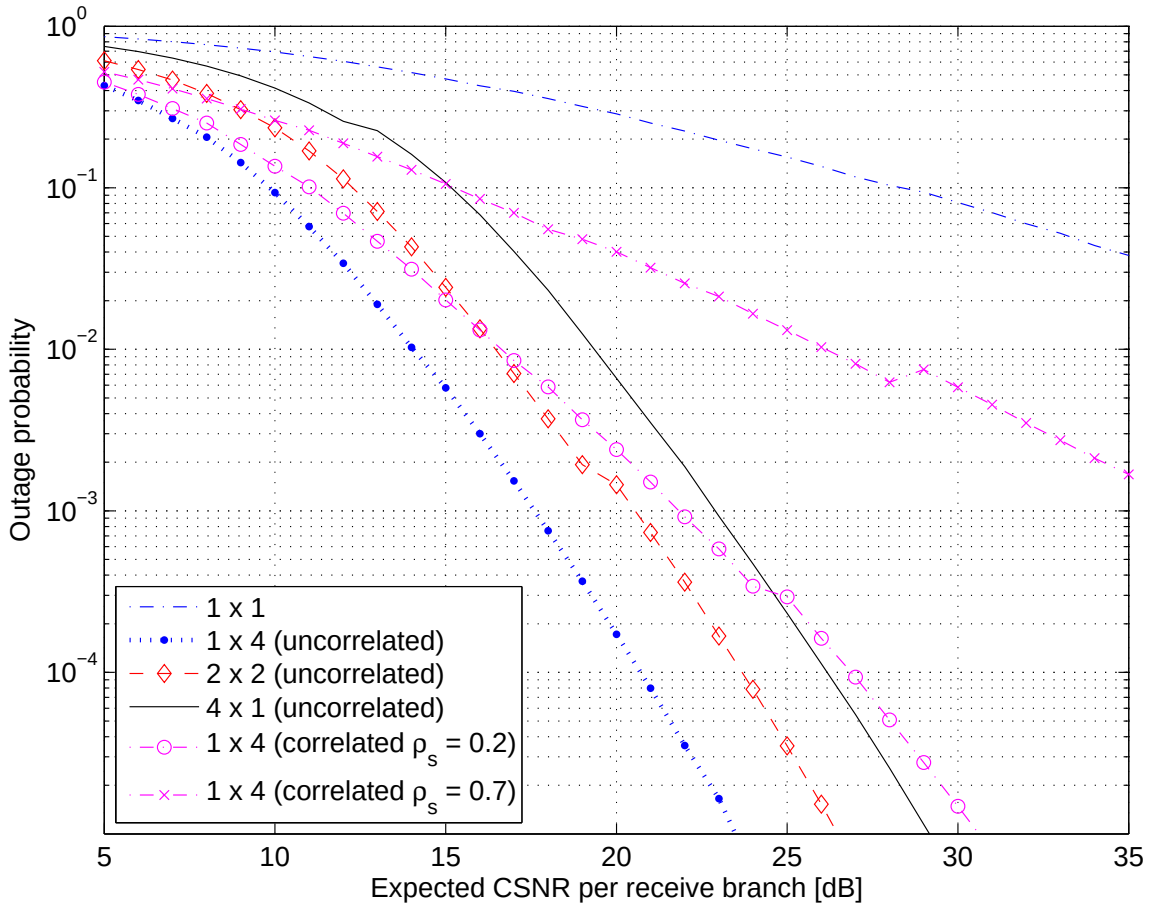

Figure 9.3: Outage probability depicted for optimal L and optimal power allocation. It is plotted as a function of average CSNR on each branch and different combinations of transmit-receive antennas.

Shown in Figure 9.3 are the curves for outage probability for different $n_{\mathrm{T}} \times n_{\mathrm{R}}$ combinations. For a fixed radiated power constraint—which is the case for the analysis in this report—clearly, the SIMO system gives lower outage probability. Thus, it is preferable to the MISO system with the same diversity order $n_{\mathrm{T}} \times n_{\mathrm{R}}$. This conclusion was also drawn from an ASE point of view in Figure 8.2, since the ASE is considerably larger in a SIMO system compared to a MISO system for the same product $n_{\mathrm{T}} \times n_{\mathrm{R}}$. In the uncorrelated branches system and with the same diversity order, probability of outage suffers a 3-dB loss for each doubling of the number of transmit antenna. This performance penalty will disappear if we double the transmit power with the doubling of the number of transmit antennas [11].

Moreover, spatial correlation gives rise to degradation of diversity gain. As shown in Figure 9.3 the curves for correlated receive antennas in a 1×4 system reduce gradually to the 1×1 system with increasing ρ_s. Note that, as with the ASE performance, it will never coincide with the 1×1 scenario due to the array gain.

10 Concluding Remarks

We have analyzed and optimized an ACM system operating on a spatial diversity channel. Both the spatially uncorrelated and correlated cases were considered. For the uncorrelated MIMO diversity case, the throughput in terms of ASE, when the transmitter is equipped with 2 antennas, outperforms the same system with only one transmit antenna. This is due to the diversity gain and to the fact that the employed orthogonal design for STBC has full rate (rate 1). This result is in contrast to what was obtained in [14] which is due to the optimization of pilot period and power performed in the present work. Having more than 2 transmit antennas gives even higher diversity order, but the overall rate is reduced due to the rate loss of the employed space-time block code.

In conclusion, for a fixed product $n_{\mathrm{T}} \times n_{\mathrm{R}}$ (the same diversity order), the ASE is still always highest for $n_{\mathrm{T}} = 1$. This indicates that when ACM is used, it is best to exploit spatial diversity by means of multiple receive antennas. In this case, even with high mobile terminal speeds, the system is, on the average, using the same constellation a reasonably long time before switching to another constellation (cf. [29, Tab. I]).

For the correlated SIMO case, the analyis is done based on separability of the space-time correlation function, i.e. representing it as a product of spatial and temporal correlation functions. Furthermore, the combined instantaneous and predicted CSNRs are approximated as gamma distributed RVs with the two first moments equal to the exact PDF.

First, we consider a suboptimal prediction procedure where the fact that the branches are correlated is not taken into account. In other words, it is the case where we use the system originally designed for spatially uncorrelated branches in a correlated one. We then predict the branches jointly where the spatial correlation is incorporated. In general, the throughput in terms of ASE is reduced due to the reduced diversity gain when spatial correlation increases. After applying the new space-time predictor it is observed that ASE is still lower than in the uncorrelated case, but the negative impact of spatial correlation on the ASE is substantially reduced. Thus, the spatial correlation should be exploited to achieve higher spectral effienciies.

References

[1] D. V. Duong. *Analysis and Optimization of Pilot-Aided Adaptive Coded Modulation Under Noisy Channel State Information and Antenna Diversity*. PhD thesis, Norwegian University of Science and Technology, 2006. Available at: `www.iet.ntnu.no/projects/beats/theses.htm`.

[2] T. S. Rappaport. *Wireless Communications Principles & Practice*. Prentice Hall, 2 edition, 2002.

[3] H. Meyr, M. Moeneclaey, and S. A. Fechtel. *Digital Communication Receivers: Synchroniza-*

tion, Channel Estimation and Signal Processing. John Wiley & Sons, 1998.

[4] W. C. Jakes. *Microwave Mobile Communications*. An IEEE Press Classic Reissue, New Jersey: IEEE Press, 1994.

[5] L. C. Godara. Applications of antenna arrays to mobile communications, part I: performance improvement, feasibility, and system considerations. *Proc. of the IEEE*, 85(7):1031–1060, July 1997.

[6] L. C. Godara. Application of antenna arrays to mobile communications, part II: beam-forming and direction-of-arrival considerations. *Proc. of the IEEE*, 85(8):1195–1245, August 1997.

[7] S. A. Jafar and A. Goldsmith. On optimality of beamforming for multiple antenna systems with imperfect feedback. In *Proc. IEEE International Symposium on Information Theory*, page 321, Washington DC, USA, June 2001.

[8] S. A. Jafar, S. Vishwanath, and A. Goldsmith. Channel capacity and beamforming for multiple transmit and receive antennas with covariance feedback. In *Proc. IEEE International Conference on Communications (ICC)*, pages 2266–2270, Helsinki, Finland, June 2001.

[9] S. Zhou and G. B. Giannakis. Optimal transmitter eigen-beamforming and space-time block coding based on channel mean feedback. *IEEE Transactions on Signal Processing*, 50(10):2599–2613, October 2002.

[10] S. Zhou and G. B. Giannakis. Adaptive modulation for multi-antenna transmissions with channel mean feedback. *IEEE Transactions on Wireless Communications*, 3(5):1626–1636, September 2004.

[11] S. M. Alamouti. A simple transmit diversity technique for wireless communications. *IEEE Journal on Selected Areas in Communications*, 16(8):1451–1458, October 1998.

[12] V. Tarokh, H. Jafarkhami, and A. R. Calderbank. Space-time block codes from orthogonal designs. *IEEE Transactions on Information Theory*, 45(5):1456–1467, July 1999.

[13] A. Paulraj, R. Nabar, and D. Gore. *Introduction to Space-Time Wireless Communications*. Cambridge University Press, 2003.

[14] B. Holter, G. E. Øien, K. J. Hole, and H. Holm. Limitations in spectral efficiency of a rate adaptive MIMO system utilizing pilot-aided channel prediction. In *Proc. IEEE Vehicular Technology Conference (VTC-Spring)*, Jeju, Korea, April 2003.

[15] S. Zhou and G. B. Giannakis. How accurate channel prediction needs to be for transmit-beamforming with adaptive modulation over Rayleigh MIMO channels? *IEEE Transactions on Wireless Communications*, 3(4):1285–1294, July 2004.

[16] K. J. Hole, H. Holm, and G. E. Øien. Adaptive multi-dimensional coded modulation over flat fading channels. *IEEE Journal on Selected Areas in Communications*, 18(7):1153–1158, July 2000.

[17] I. S. Gradshteyn and I. M. Ryzhik. *Table of Integrals, Series and Products*. Academic Press, 6 edition, 2000.

[18] Y. Ko and C. Tepedelenlioglu. Orthogonal space-time block coded rate-adaptive modulation with outdated feedback. *IEEE Transactions on Wireless Communications*, 5(2):290–295, February 2006.

[19] X. Cai and G. B. Giannakis. Adaptive PSAM accounting for channel estimation and prediction errors. *IEEE Transactions on Wireless Communications*, 4(1):246–256, January 2005.

[20] J. K. Cavers. An analysis of pilot symbol assisted modulation for Rayleigh fading channels. *IEEE Transactions on Vehicular Technology*, 40(4):686–693, November 1991.

[21] G. E. Øien, R. K. Hansen, D. V. Duong, H. Holm, and K. J. Hole. Bit error rate analysis of adaptive coded modulation with mismatched and complexity-limited channel prediction. In *Proc. IEEE Nordic Signal Processing Symposium (NORSIG)*, Hurtigruten, Norway, October 2002.

[22] S. Sandhu and A. Paulraj. Space-time block codes: A capacity perspective. *IEEE Communication Letters*, 4(12):384–386, December 2000.

[23] Y. Ko and C. Tepedelenlioglu. Space-time block coded rate-adaptive modulation with uncertain SNR feedback. In *Proc. Asilomar Conference On Systems and Computers*, November 2003.

[24] Y. Ko and C. Tepedelenlioglu. Optimal switching thresholds for space-time block coded rate-adaptive M-QAM. In *Proc. IEEE International Conference on Acoustics, Speech and Signal Processing (ICASSP)*, Montreal, Canada, May 2004.

[25] J. M. Torrance and L. Hanzo. Optimisation of switching levels for adaptive modulation in slow Rayleigh fading. *IEE Electronics Letters*, 32(13):1167–1169, June 1996.

[26] L. Hanzo, M. Münster, B. J. Choi, and T. Keller. *OFDM and MC-CDMA for Broadcasting Multi-User Communications, WLANs and Broadcasting*. John Wiley & Sons, 2003.

[27] J. H. Winters. Smart antennas for wireless systems. *IEEE Personal Communications*, 5:23–27, February 1998.

[28] T. Ratnarajah. Spatially correlated multiple-antenna channel capacity distributions. *IEE Proceedings-Communications*, 153(2):263–271, April 2006.

[29] D. V. Duong and G. E. Øien. Optimal pilot spacing and power in rate-adaptive MIMO diversity system with imperfect CSI. *IEEE Transactions on Wireless Communications*, 6(3), March 2007.